Determination of the Mode I Fracture Toughness and Tensile Strength of Compacted Clays

Keda Cao & Ron Chik-Kwong Wong
Department of Civil Engineering – University of Calgary, Calgary, Alberta, Canada

ABSTRACT
An understanding of tensile properties of geomaterials is important to control the formation and propagation of tensile cracks in geotechnical structures. Tensile strength σ_t and fracture toughness K_{Ic} are two parameters used to define the ability of resisting fracture under tensile stresses (mode I). In this study, K_{Ic} and σ_t of two clays were measured by straight notched disk bending (SNDB) method and uniaxial direct tensile test respectively. For Calgary till, K_{Ic} of specimens with same dry density increases with decreasing moisture content within the test range; for Regina clay, of which the samples were compacted with consistent compaction energy, the values show a peak when moisture content goes down. The changing trends of σ_t are very similar with K_{Ic}, hence there is a strong positive correlation between tensile strength and fracture toughness.

RÉSUMÉ
Une compréhension des propriétés en traction des matériaux géotechniques est importante pour contrôler la formation ainsi que la propagation des fissures dues à la traction dans les structures géotechniques. La résistance à la traction σ_t et la ténacité à la rupture K_{Ic} sont deux paramètres utilisés pour définir la capacité de résistance à la rupture sous des contraintes de traction (mode I). Dans la présente étude, K_{Ic} et σ_t de deux argiles ont été mesurés par la méthode de cintrage à disque dentelé droit (SNDB en anglais) et par l'essai de traction directe uniaxiale respectivement. D'après Calgary till, le K_{Ic} des échantillons ayant la même masse volumique sèche augmente lorsque la teneur en eau diminue dans la plage d'essai; pour Regina clay, dont les échantillons ont été compactés avec une énergie de compactage constante, la courbe des valeurs présente un sommet lorsque le taux d'humidité diminue. Les tendances de variation de σ_t sont très similaires à celles de K_{Ic}. Par conséquent, il existe une forte corrélation positive entre la résistance à la traction et la ténacité à la rupture.

1 INTRODUCTION

Attention has been increasingly paid to tensile properties of geomaterials since the existence of tensile cracks could potentially cause structure failure, such as landslide induced by crack extension at the crest of a slope, clay-liner leakage because of desiccation cracks and earth dam failure due to crack propagation within the dam core (Miller et al., 1998; Li & Yang, 2016; Wang et al., 2016). The interest in how cracks would appear in geomaterials has been aroused in past decades.

To characterize cracking behaviours of soils, from the perspective of classic strength-of-material approach, tensile strength is usually used to describe the ultimate stress that the material can bear. This property has been extensively investigated and applied in engineering practices. Nonetheless, as a matter of fact, cracks are quite easy to be generated when structures are subjected to temperature variation, moisture loss or stress state change. Once cracks exist in those structures, even very small cracks, the stress field distribution under loads will change significantly because stresses tend to concentrate on crack tips, which possibly leads to crack extension and ensuing ultimate structure failure. Though the classic tensile strength is able to define the condition for crack initiation, it will not be capable to predict the crack propagation process, which should be described by fracture mechanics instead.

Tentatively, Linear Elastic Fracture Mechanics (LEFM) has been adopted to investigate the cracking behaviours of soils (e.g. Wang et al. 2007). In LEFM, the state of stress concentration at a crack tip is defined by stress intensity factor K_I. Only if K_I reaches a critical value, the crack extends. This critical value is considered as a mechanical property called fracture toughness K_{Ic} which reflects the ability of resisting fracturing under tensile loads (Mode I opening) for brittle or quasi-brittle materials. The determination of K_{Ic} will give the critical state at which a crack is going to extend.

In this study tensile properties of both fracture toughness and tensile strength were investigated. The fracture toughness of clays was measured by a method originally for rocks, named Straight Notched Disk Bending (SNDB), which is applied to soils for the first time in this investigation due to its simplicity of sample preparation and experimental setup. Tensile strength was obtained through uniaxial direct tensile test with common dog-bone shape specimens. Two types of clays, Calgary till and Regina clay, were tested to examine the influences of moisture content and dry density on the variations of K_{Ic} and σ_t. For these two properties, it was found previously in other researches that K_{Ic} was positively correlated to σ_t for geomaterials but the correlation was still uncertain, possibly a linear or power law. So their relationship was also checked in this research.

This paper presents the fracture toughness test procedures and results first, then uniaxial direct tensile tests, and finally the correlation between the two tensile properties.

2 CLAY PROPERTIES

Two types of soils used in the investigation were collected from the construction sites. Calgary till was obtained from Sage Hill in Calgary, Alberta, whilst Regina clay was excavated near Mosaic Stadium in Regina, Saskatchewan, Canada. Prior to the tests, all of impurities, like leaves and branches, were picked out, then the soils were air-dried, pulverized, and sieved through a 2 mm sieve.

Basic properties including Atterberg Limits, soil classifications, clay contents, optimum dry densities with corresponding moisture contents under standard proctor, and specific gravities of two clays are listed in Table 1.

Table 1. Basic properties of two tested clays

Properties	Calgary till	Regina clay
Liquid Limit (LL)	37%	69%
Plastic Limit (PL)	19%	29%
Plastic Index (PI)	18%	40%
Clay Content	15%	50%
Classification	CL	CH
Optimum Dry Density ($\rho_{d,\,max}$)	1.50 g/cm^3	1.85 g/cm^3
Optimum Moisture Content (w_0)	15%	25%
Specific Gravity (G_s)	2.75	2.83

3 FRACTURE TOUGHNESS

To obtain Mode I fracture toughness, a crack must extend under tensile stresses. The tensile-stress state could be generated by three-point bending. SNDB method, firstly developed by Alkilicgil (2006) for testing K_{Ic} of rocks, is a type of three-point bending assembly where a loading rod applies compressive load on the top and two rollers at the bottom support the specimen. A crack is machined throughout the diameter at the bottom surface of the disk specimen. The fixture and specimen geometry are presented in Figure 1, where P is the load exerting on the loading rod, S is the length of half span, D is the diameter of the disk, R is the radius, t is the thickness, and a is the crack depth.

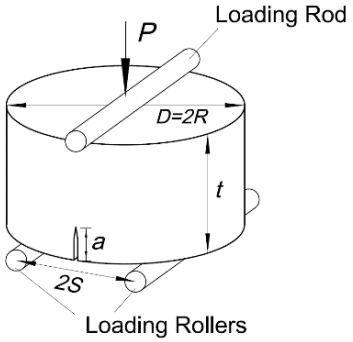

Figure 1. SNDB geometries and fixture

The crack opens when the compressive force P increases gradually. The crack would propagate once the stress intensity factor at the crack tip approaches the critical value meanwhile the compressive force reaches a maximum value. This critical stress intensity factor calculated from the maximum compressive load P_{max} is the fracture toughness of the specimen.

3.1 Test Setup

The experiments are conducted on a load frame where all the instruments are mounted on. The experimental setup is seen from Figure 2: an adaptor that holds the loading rod is installed on the load cell, and in between the adaptor and the load cell is a balance strip that helps LVDTs reduce measurement error induced from rotation. Two same LVDTs are placed symmetrically on both sides, making sure the symmetry as the measured displacements will be corrected by taking the average of the two. The specimen is loaded by the upper loading rod and the lower loading rollers that are supported by bearings. The size of bearings just fits the loading rollers, to prevent rollers from waggling and to ensure smooth rotation with very small friction. Bearings are fixed tightly on supporters with fixtures, while supporters are immobilized on the base with screws. After assembling, the integrality of the parts connected to the base and the horizontal mobility of the load cell must be checked so that the desired three-point bending could be realized.

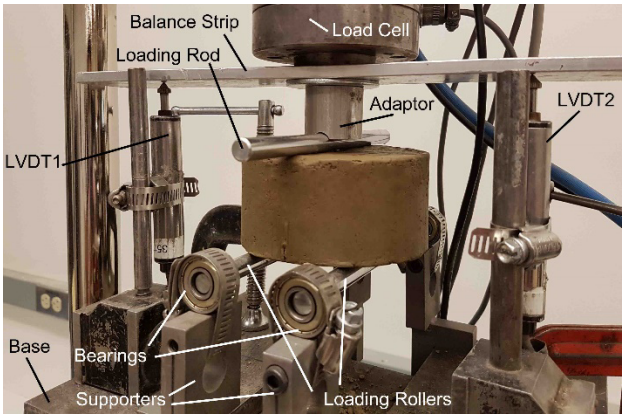

Figure 2. Experimental setup of SNDB

3.2 Calculation on K_{Ic}

For the calculation of K_{Ic}, Tutluoglu & Keles (2011) offered Equations 1 & 2 derived from finite element modeling. The parameters in the equations change with specimen geometries a/t, t/R and S/R. Not all of geometry ratios give effective solutions for fracture toughness computation. When $t/R > 2.0$ and $S/R < 0.4$, or $a/t < 0.5$ and $S/R < 0.4$, the stress intensity factor appears to be negative, which means it is compressive stresses that distribute around the crack tip rather than tensile stresses. Hence, it is preferable that $S/R \geq 0.5$ and the stress intensity factor Y_I can be expressed as a function of m, n and S/R, where m and n can be found in Table 2 according to the geometries.

Because the specimens of this study are compacted in the collar of standard compaction mold used in ASTM

D698 (Figure 3), of which t/R = 1.0 and D = 101.6 mm (4 inches), only t/R = 1.0 scenario is given in Table 2.

$$K_{Ic} = Y_I \frac{P_{max}}{2Dt}\sqrt{\pi a} \quad [1]$$

$$Y_I = m(S/R) + n \quad [2]$$

Table 2. Values of m and n for stress intensity factor estimation for t/R = 1.0 specimen (after Tutluoglu & Keles 2011)

a/t	m	n
0.1	5.2801	0.1421
0.2	5.8903	-0.4229
0.3	6.5884	-0.7633
0.4	7.4728	-0.9269
0.5	8.8301	-0.9966

Figure 3. Compaction mold for the specimens

3.3 Test Procedures

Sample preparation and experiment conduction are the main stages of testing procedures. The tests were conducted according to the following steps:

Oven-dried and pulverized soils are fully mixed with water to pre-determined water contents and then sealed in air-tight zip-lock bags for at least three days for moisture equilibrium. Before compaction, the mass of specimen is calculated through the volume of compaction mold and the desired density so that the needed soil could be weighed and subsequently compacted using a standard compaction hammer. The number of blows of the compaction hammer is dependent on the moisture content and dry density of the specimen and is obtained from the author's experience. The required number of blows is listed in Table 3. After compaction, the upper surface of the specimen should be flattened by knife and small hammer.

After compaction, careful sawing is followed immediately, for which a commercial 101.60 mm (4 inches) miter box is used to help guide the hand saw (Figure 4) to make sure the notch is straight and to avoid disturbance to the sample. The width of saw is about 0.5 mm, which will make a 1.0 mm wide notch for the specimen after sawing.

The notched sample must be sealed by plastic film immediately to prevent moisture loss and stored in a sealed bag, standing for at least 24 hours to eliminate excess pore pressure induced by compaction and sawing (Figure 5).

Before conducting the experiment, firstly, the specimen should be carefully inspected visually to identify any additional cracks that possibly occur in the specimen body during standing; if none, the specimen is placed on the apparatus as shown in Figure 2. Loading rate is set to 0.2 mm/min, recommended by Kuruppu et al. (2013) on the purpose of avoiding any dynamic effects. Readings of displacement gauges and load cell are recorded by a computer program simultaneously at the frequency of 2HZ. At this rate of loading, each test shall finish in 15 minutes so that moisture loss could be controlled to an acceptable extent. Vertical cracking propagation is expected to be observed when the load achieves the maximum.

Moisture content should be checked after the test and compared with the pre-test value. The periphery of the sample, where moisture loss could be significant during the test, is cut and only the core is used for moisture measurement. At least 200 g soil was collected and oven-dried for 24 hours. Moisture loss less than 0.5% for a single specimen was observed, which is considered reasonably acceptable for such specimen size.

Figure 4. Sawing the specimen with hand saw guided by miter box

(a) (b)

Figure 5. Standing specimens (a) wrapped by plastic film (b) sealed in zip-lock bag

3.4 Test Program

Specimens of Calgary till were compacted to two different dry densities 1.75 g/cm^3 and 1.85 g/cm^3, with moisture contents from 11% to 19.5% for 1.75 g/cm^3 and

w = 11% - 17% for 1.85 g/cm^3 scenarios, whilst specimens of Regina clay were compacted by using same compaction energy so that the values of w and ρ_d were located on the compaction curve over the range of w = 19.5% - 31%. The numbers of blows for specimens with different moisture contents and dry densities are listed in Table 3 as well. Specimens with moisture contents lower than the ranges were too fragile to saw and higher ranges were too soft to prepare. The notch length was limited to 10 mm at a ratio of a/t = 0.2 for all of the specimens, which was easy to saw within a short time and less possible to induce sample disturbance. One or two specimens were prepared for each moisture content in this preliminary research. The testing scheme is present in Table 3, which were also used for the direct tensile tests later. What's more, due to the weak strength of materials, to minimize the self-weight effect, S/R = 0.5 for Calgary till and S/R = 0.6 for Regina clay were used as suggested by Kuruppu et al. (2013).

Table 3. Testing scheme of K_{Ic} for two compacted clays and required blows for compaction

	a (mm)	a/t	ρ_d (g/cm^3)	w (%)	Number of blows
Calgary till	10	0.2	1.75	11	10
				13	8
				15	6
				17	8
				19.5	10
			1.85	11	16
				13	14
				15	10
				17	14
Regina clay	10	0.2	1.45	19.5	10
			1.48	22	
			1.50	25	
			1.48	28.5	
			1.45	31	

3.5 Test Results

The load P and load-point displacement were recorded over the range of both pre-peak and post-peak stages. The fracture toughness K_{Ic} was calculated from the peak load maximum P_{max} if it was considered that P_{max} is the critical force that initiates crack propagation.

Typical load-displacement curves of Calgary till and Regina clay are present in Figure 6, from which obvious peaks could be observed and each curve could be divided into three stages: run-in stage; loading stage; post-peak stage. Run-in stage is commonly seen from all kinds of load-displacement curves, at which the loading parts in the system are still loosely assembled; after running in, the curve enters a loading stage where the compressive load hikes steadily until it approaches the peak; subsequently, the critical load initiates crack extension rapidly. From typical curves, it could be seen there is a tendency that curves of lower moisture content specimens have less post-peak points, which means the specimens fail more quickly after the critical load as these points are recorded at the same frequency. Thus lower moisture specimens could be deemed more brittle. Besides, another regularity is apparent that samples having higher failure loads have steeper slopes, reflecting the fact that the stronger the strength is the stiffer the sample will be. These slopes can be references for numerically modelling the fracturing behaviours of soils with different dry densities and moisture contents.

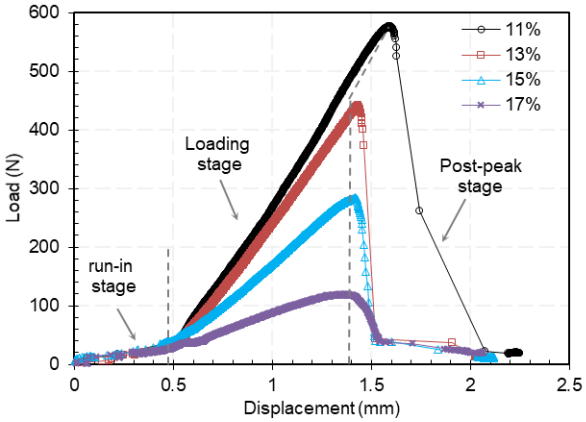

Figure 6. Typical load-displacement curves of SNDB tests of (a) Calgary till, ρ_d = 1.85 g/cm^3 (b) Regina clay

From peak loads, values of fracture toughness could be gained through Equation 1 & 2. Obtained K_{Ic} of the two clays following the testing program are shown in Figure 7. As to Calgary till, a decrease of moisture content leads to an increase of K_{Ic}; two distinct data bands of two densities appear. As to Regina clay, an increasing-decreasing curve of K_{Ic} variation was found with a peak at w = 22%; this is of interest because the matrix suction, which is considered as the main contribution of the strength of unsaturated soil, goes up when moisture content declines.

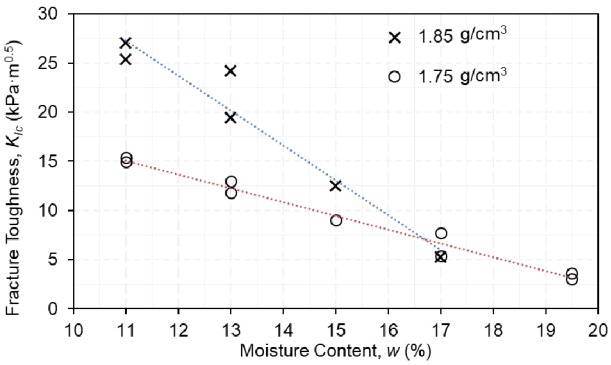

(a)

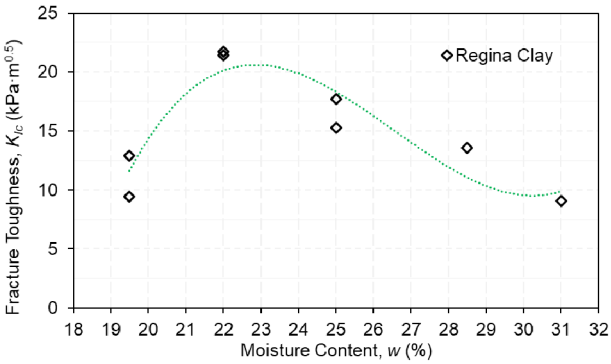

(b)

Figure 7. Variations of K_{Ic} with respect to moisture content of (a) Calgary till; (b) Regina clay

4 UNIAXIAL TENSILE STRENGTH

4.1 Test Setup and Procedures

Figure 8 shows the loading assembly and the apparatus. The apparatus include, two clamps holding the dog-bone specimen, a spring gauge installed on the clamps for recording the displacement, and wire ropes connecting the load cell and the base to the clamps.

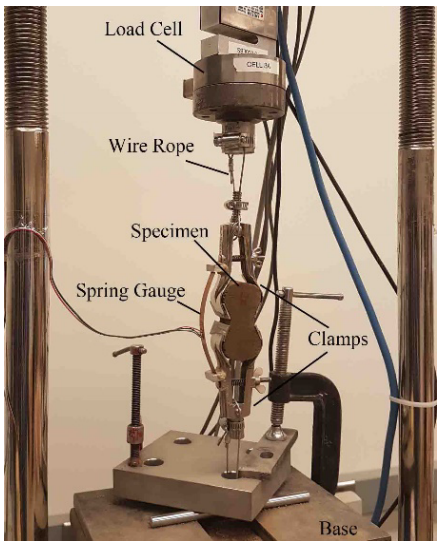

Figure 8. Setup of uniaxial tensile test

Figure 9. Compacted dog-bone specimen in the mold

According to the test setup, tensile strength could be calculated from Equation 3. The weight of upper half of specimen and the upper clamp should be subtracted from the maximum force measured by the load cell.

$$\sigma_t = \frac{F_{max} - W}{A} \quad [3]$$

Where F_{max} = failure load measured by the load cell; W = the total weight of the upper half of specimen and the upper clamp; A = cross-section area of specimen neck (25.16 mm × 25.55 mm)

The testing program was exactly same as K_{Ic} tests as listed in Table 3. After standing, soils with required moisture contents were prepared in the same way as K_{Ic} test, and then compacted in a dog-bone mold (as Figure 9) in one layer to the pre-determined dry density using a small hammer. The required mass of soil for compaction was calculated from the moisture content and dry density of specimen, and the volume of compaction mold. Specimens were wrapped with cling wrap and stored in air-tight bags as well for 24 hours prior to tests. Loading rate was 0.2 mm/min and data acquisition frequency was 10 points per second. Moisture content was checked afterwards each test using the whole specimen. Reasonable moisture losses less than 0.5% were observed.

4.2 Test Results

Typical load-displacement curves of tensile tests for Calgary till and Regina clay are shown in Figure 10. Higher moisture contents result in more significant post-peak softening; for instance, w = 17% of Calgary till has up to 0.36 mm post-peak elongation at the specimen neck but w = 11% only has less than 0.04 mm. This is due to the increase of ductility alongside increasing moisture content.

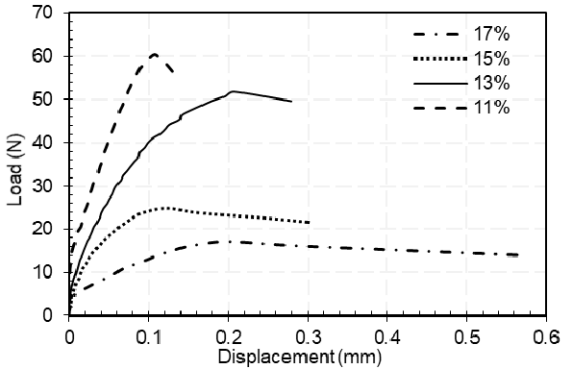

(a)

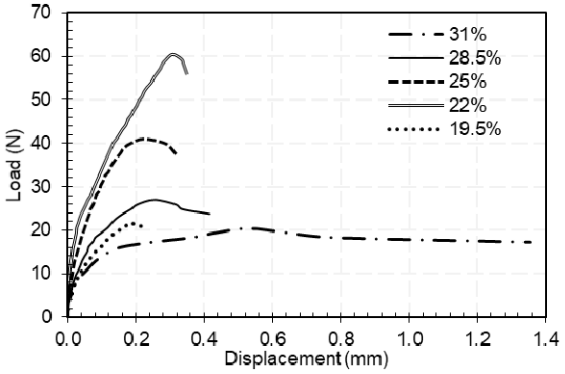

(b)

Figure 10. Typical load-displacement curves of uniaxial tensile tests of (a) Calgary till, ρ_d = 1.85 g/cm^3 (b) Regina clay

Interestingly, the changing trends in Figure 11 of tensile strength are almost identical to K_{Ic}: two clear increasing trends dependent on dry densities appear for Calgary till; an exactly same variation is found for Regina clay where a peak shows at w = 22%. As the changes of tensile strength and fracture toughness along with dry densities and moisture contents are so similar, it is possible to correlate these two mechanical parameters somehow.

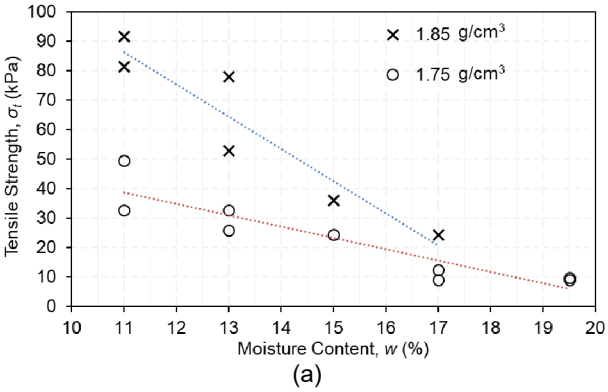

(a)

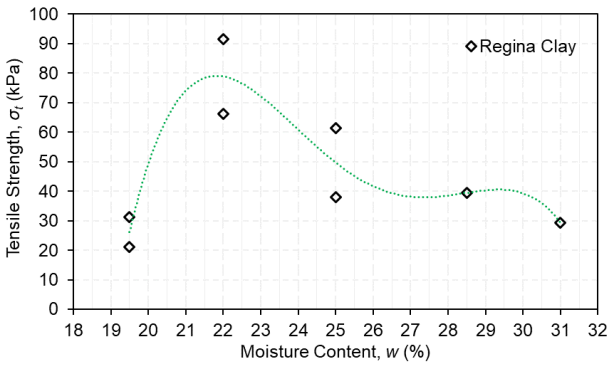

(b)

Figure 11. Variations of tensile strength of (a) Calgary till; (b) Regina clay

5 RELATIONSHIP BETWEEN TENSILE STRENGTH AND FRACTURE TOUGHNESS

Empirical correlations between the two properties were mostly found linear or power-law for different types of rocks (e.g. Haberfield & Johnston, 1989). But for the correlation of compacted clays, only limited cases are available.

Harison et al. (1994) investigated the relationship for the first time using compacted ring test specimens and present a strong linear correlation; Wang et al., (2007) developed a horizontal loading system of Single Edge Notched Bending (SENB) method for K_{Ic} and obtained a reasonable linear relation with σ_t obtained from uniaxial tensile test; Amarasiri & Kodikara (2011) determined K_{Ic} using SENB, then gained the corresponding tensile strength through numerical modelling, from which both good linear and power-law relationships were found; Lakshmikantha et al. (2012) used Compact Tension (CT) method and direct tensile test to study the parameters but few of the data could be used for a correlation. Thus far, the correlation is still uncertain for compacted clays.

The fracture toughness obtained in this preliminary study are plotted in Figure 12, against the tensile strength one-to-one according to the sequence of tests. Curve fitting gives the coefficients of determination R^2 = 0.7127 and R^2 = 0.7889 for linear Equation 4 and power-law Equation 5 respectively. The coefficient of determination of power-law is slightly higher, which is in line with the observation of Amarasiri & Kodikara (2011). The coefficients of determination in this preliminary study are not high enough to show a very strong relation, even though a positively correlated trend exhibits. For further investigations later, more specimens should be tested so that the sample space is sufficiently large to present the relationship between the properties.

$$K_{Ic} = 0.3519\sigma_t \quad [4]$$

$$K_{Ic} = 0.8383\,\sigma_t^{0.7879} \quad [5]$$

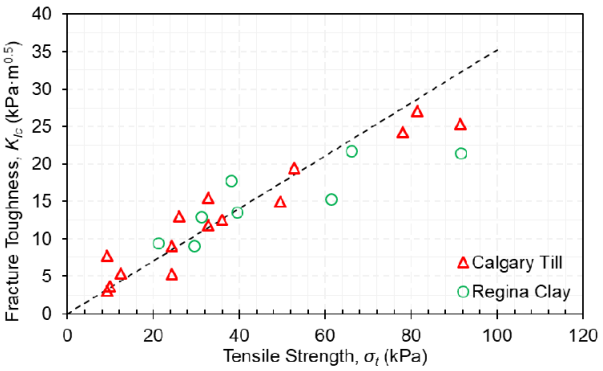

(a)

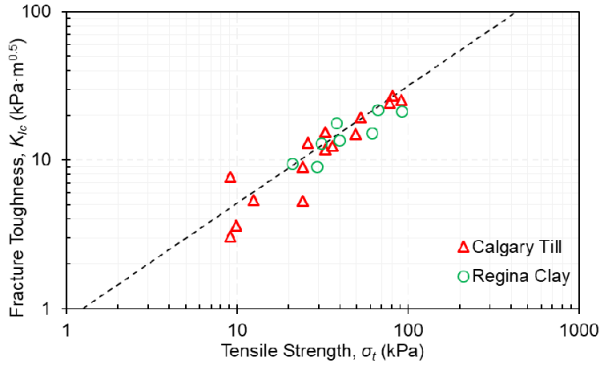

(b)

Figure 12. (a) Linear and (b) power-law correlations for the two clays

6 CONCLUSION

SNDB and uniaxial direct tensile tests were used in this preliminary study to screen the cohesive properties, mode I fracture toughness K_{Ic} and tensile strength σ_t, of two compacted clays. It showed that for Calgary till compacted to constant densities, values of K_{Ic} were higher at lower moisture contents, and larger dry density contributed to larger K_{Ic}; for Regina clay compacted under constant compaction energy, a peak value was found when moisture content drops down from the dry of optimum to the wet side. Similar variations of σ_t and K_{Ic} of both clays were found, so a strong correlation between them is supposed to exist. The data in this study revealed that both linear and power-law equations could reasonably fit the relationship, however, more data points are needed for a larger sample space and better correlation.

7 ACKNOWLEDGEMENT

Natural Sciences and Engineering Research Council (NSERC) and the University of Calgary are gratefully acknowledged for their financial supports to this research.

8 REFERENCES

Alkilicgil, Ç. 2006. *Development of a new method for mode I fracture toughness test on disc type rock specimens*, Master's thesis, Middle East Technical University, Ankara, Turkey.

Amarasiri, A.L. and Kodikara, J.K. 2011. Determination of cohesive properties for mode I fracture from beams of soft rock, *International Journal of Rock Mechanics and Mining Sciences*, 48(2): 336–340.

Haberfield, C. and Johnston, I. 1989. Relationship between fracture toughness and tensile strength for geomaterials, *12th International Conference on Soil Mechanics and Foundation Engineering*, Balkema, Rio de Janeiro, Brazil, 1: 47–52.

Harison, J.A., Hardin, B.O. and Mahboub, K. 1994. Fracture toughness of compacted cohesive soils using ring test, *Journal of Geotechnical Engineering*, 120(5): 872–891.

Kuruppu, M.D., Obara, Y., Ayatollahi, M.R., Chong, K.P. and Funatsu, T. 2013. ISRM-suggested method for determining the mode I static fracture toughness using semi-circular bend specimen, *Rock Mechanics and Rock Engineering*, 47(1): 267–274.

Lakshmikantha, M.R., Prat, P.C. and Ledesma, A. 2012. Experimental evidence of size effect in soil cracking, *Canadian Geotechnical Journal*, 49(3): 264–284.

Li, Y.X. and Yang, X.L. 2016. Stability analysis of crack slope considering nonlinearity and water pressure, *KSCE Journal of Civil Engineering*, 20(6): 2289–2296.

Miller, C.J., Mi, H. and Yesiller, N. 1998. Experimental analysis of desiccation crack propagation in clay liners, *JAWRA Journal of the American Water Resources Association*, 34(3): 677–686.

Tutluoglu, L. and Keles, C. 2011. Mode I fracture toughness determination with straight notched disk bending method, *International Journal of Rock Mechanics and Mining Sciences*, 48(8): 1248–1261.

Wang, J.-J., Zhu, J.-G., Chiu, C.F. and Zhang, H. 2007. Experimental study on fracture toughness and tensile strength of a clay, *Engineering Geology*, 94(1–2): 65–75.

Wang, J., Zhu, J., Mroueh, H. and Chiu, C. 2016. Hydraulic fracturing of rock-fill dam, *The International Journal of Multiphysics*, 1(2): 199–220.